# The Influence of a Grid-Generated Turbulence on the Development of Chemical Reactions

A. BENNANI,
J. N. GENCE, and
J. MATHIEU

Laboratoire de Mécanique des Fluides
Ecole Centrale de Lyon et Université de Lyon I
Ecully, France

The evolution of slow, irreversible, isothermal, second-order chemical reactions between two nonpremixed species is experimentally studied in a field of quasi-isotropic grid turbulence developing in a water tunnel. The experiments provide some basic data on the interaction between the turbulent mixing and the reaction, which tends to remove the mixed species.

## SCOPE

Turbulence is known to influence strongly the diffusion process and, as a result, the chemical reactions taking place in a flowing fluid mixture (Hill, 1976; Villermaux, 1982). Many experimental works concerning the influence of turbulence on mixing have been carried out in statistically inhomogeneous and nonisotropic flows, for instance, in a stirred-tank reactor. The present work was undertaken in order to satisfy the obvious need for experiments performed in conditions close enough to an ideal statistically homogeneous situation. Accordingly, the evolution of a chemical reaction in a quasi-isotropic grid-generated turbulence was studied experimentally. In order to avoid any contact of the two reacting species $A$ and $B$ upstream of the grid, one of them was injected through it, while the other was carried out by the main flow. For the sake of simplicity, the scope of the investigation was limited to the case of an irreversible second-order isothermal reaction taking place in an aqueous solution between two chemical components of identical molecular diffusivities. As indicated by Hill (1976), the behavior of the different concentration fields is a priori governed by the following three mechanisms:

1. The convection by the mean flow and the associated production and turbulent diffusion whose common characteristic time is $\tau_1 = L/\sqrt{\overline{q}^2}$. Here $\overline{q}^2$ is the kinetic energy of the fluctuating motion and $L$ the length scale of the energy containing eddies. The length $L$ is also of the order of an integral scale, which corresponds, in a given direction, to the longest distance along which the velocity fluctuations are correlated.

2. The decrease of the variance due to molecular diffusion whose time scale is $\tau_2 = \lambda^2/D$. Here $\lambda$ is of the order of Taylor's length scale and $D$ the molecular diffusivity.

3. The chemical reactions whose relaxation time is $\tau_3 = (k_r C)^{-1}$. Here $C$ is a characteristic concentration and $k_r$ the kinetic constant.

Inasmuch as the fluctuating velocity is not influenced by the chemical reaction, the turbulent flow may be characterized by the turbulent Reynolds number

$$Re_L = \frac{L\sqrt{\overline{q}^2}}{\nu}$$

$\nu$ is the kinematic viscosity, which, in the special case of a grid turbulence, is proportional to the Reynolds number based on the grid mesh $M$ and the mean velocity $\overline{U}$, (Corrsin, 1963).

From the foregoing, it is obvious that a complete description of the problem requires the introduction of the two Damköhler numbers,

$$Da_L = \tau_1/\tau_3; \quad Da_\lambda = \tau_2/\tau_3$$

In the special case considered here, the turbulence is isotropic, so that no mean velocity and concentration gradients exist and that the velocity and concentration fluctuations are not correlated. This implies that the former mechanism does not take place and only the variations of $Da_\lambda$ need be considered. Actually, two situations were investigated:

$$Da_\lambda < 1$$

corresponding to a very slow reaction in which the controlling mechanism is the molecular destruction of variance, and

$$Da_\lambda > 1$$

which makes it possible to observe the influence of the chemical reaction on the behavior of the concentration fields. In addition, the reference case of a passive scalar associated with a vanishing Damköhler number was studied.

Correspondence concerning this paper should be directed to J. N. Gence.

## CONCLUSIONS AND SIGNIFICANCE

As found by Gibson (1962), the variance of a passive concentration field in a quasiisotropic grid turbulence exhibits a power law of decay that agrees well with that observed in the case of fluctuations of a passive temperature field in the same flow conditions.

When a very slow reaction is considered, the behavior of the mean concentration fields is very similar to the one expected in an ideal plug-flow reactor so that the correlation $c_A c_B$ can be neglected against the product $\bar{C}_A \cdot \bar{C}_B$ at a distance far enough from the injectors, the characteristic time of mixing being much smaller than the time of reaction.

When a faster reaction takes place, the ratio $-\overline{c_A c_B}/\bar{C}_A \cdot \bar{C}_B$ rapidly reaches a constant value of about 0.7 as a result of an equilibrium between two competitive mechanisms: the destruction of $|\overline{c_A c_B}|$ by molecular diffusion and the growth of $|\overline{c_A c_B}|$ due to the chemical reaction, which tends to prevent the species to coexist. Moreover, it is worthwhile noting that the decay of $|\overline{c_A c_B}|$ and of the variance of a passive concentration are quite similar, in agreement with the prediction of Toor's (1969) model.

## EXPERIMENTAL

### Setup

The test tunnel is a 2 m long, 0.3 m dia cylinder, (Figure 1a). The measurement probes penetrate the tunnel through different holes located every 20 cm along the streamwise direction.

The grid, which generates the turbulence, has a square 3.5 cm mesh $M$, and its solidity is equal to 0.36 (the solidity is defined as the ratio of the surface of the grid to the surface of the section of the test tunnel). Many (272) 1.5 cm long injectors are regularly distributed along the different rods of the grid (Figure 1b). The flow rate through the injectors is regulated by taps in order to obtain better homogeneity downstream. Such a setup has already been used by several authors, in particular by Gibson (1962) with a water flow, and Alcaraz and Mathieu (1965) and Gad El Hak and Corrsin (1974) with an air flow.

The whole facility, which has been extensively described by Bennani et al. (1981) is composed of two circuits, depicted in Figure 1a:

- A main circuit in which a solution of one of the two reacting species flows through the grid.
- A secondary circuit through which a solution of the other species is injected in the grid section.

Since the products of the chemical reactions have to be eliminated, the main flow results from the discharge of a tank I containing the solution flowing through the grid (Figure 1a), the products of the reaction being stored in a second tank II during the process. A pump, whose rotation is controlled by the head of tank I, provides a constant mean velocity in the tunnel during a time interval of about 50 s, which is long enough for the data acquisition.

### Measurement Methods

The velocity fluctuations are determined by use of a classical X-hot-film probe DISA connected to a DISA 55D01 constant temperature anemometer associated with a DISA 55D25 unit.

One of the reactants is ionic, so that the measurement of its concentration fluctuations is made by use of a conductimetric probe described by Gibson and Schwartz (1963). They have shown, in particular, that the attenuation of the measured concentration fluctuations by such a probe of characteristic radius $\mathcal{D}$ is of 10% when the spatial wavelength is about 50 $\mathcal{D}$. In the present experiment, $\mathcal{D} = 50\ \mu$m, so that the spatial wavelengths, which can be measured with good accuracy, are greater than 2 mm. It is easy to show (Tennekes and Lumley, 1972, p. 96) that if $\lambda_c$ and $\lambda_g$ are, respectively, the Taylor microscales associated with the concentration and velocity fluctuations, we have

$$\lambda_c/\lambda_g = \alpha' \sqrt{\frac{D}{\nu}} = \alpha'(Sc)^{-1/2}, \tag{1}$$

where $Sc$ is the Schmidt number and $\alpha'$ a constant of order 1. In the present experiment $\lambda g$ is about 4 mm and $Sc$ about 700, so that $\lambda_c \simeq 0.15$ mm, which is impossible to measure with such a conductimetric probe.

Another limitation of such probes is that they are sensitive to the fluctuations of all the ions in the solution. More precisely, if the flow is a diluted solution containing $N$ ions whose charge, mobility, and concentration are, respectively, $z_\alpha$, $\gamma_\alpha$, and $\mathcal{C}_\alpha$, a perfectly local probe would measure the local conductivity $\Gamma$, given by

$$\Gamma(\vec{x},t) = K \sum_\alpha \gamma_\alpha |z_\alpha| \mathcal{C}_\alpha(\vec{x},t), \tag{2}$$

where $K$ is a constant.

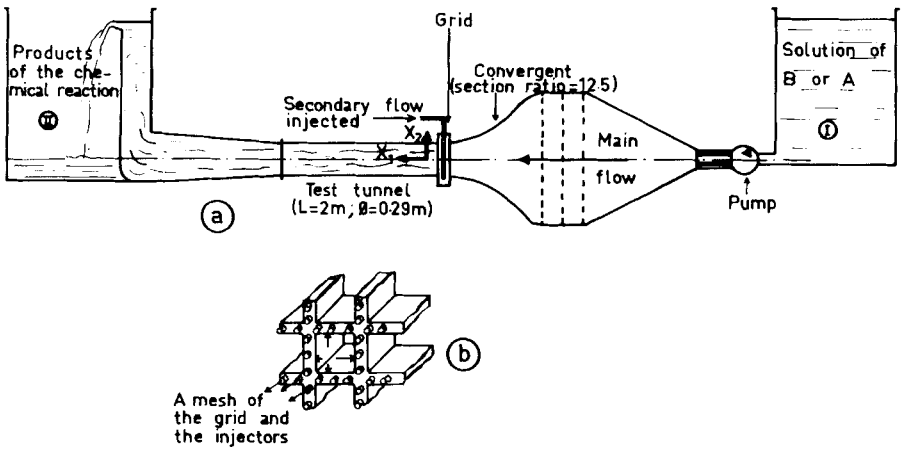


**Figure 1. (a) Scheme of the experimental setup. (b) Scheme of a mesh surrounded by injectors.**

If only one species ($A$) is diluted—as in the case discussed in the next section—where the concentration field of NaCl is a convected passive scalar, relation 2 reduces to

$$\Gamma(\vec{x},t) = k[\gamma_{Na^+}\mathcal{C}_{Na^+}(\vec{x},t) + \gamma_{Cl^-}\mathcal{C}_{Cl^-}(\vec{x},t)]. \quad (3)$$

However, charge conservation implies that

$$\mathcal{C}_{Na^+}(\vec{x},t) = \mathcal{C}_{Cl^-}(\vec{x},t) = \mathcal{C}_A(\vec{x},t), \quad (4)$$

so that

$$\Gamma(\vec{x},t) = K(\gamma_{Na^+} + \gamma_{Cl^-})\mathcal{C}_A(\vec{x},t), \quad (5)$$

and the conductimetric method may be used.

If different ionic species are diluted—as is the case in the later section on a very slow reaction—where the following isothermal chemical reaction takes place:

$$CH_3COOC_2H_5 + Na^+OH^- \rightarrow CH_3COO^-Na^+ + C_2H_5OH, \quad (6)$$

$\Gamma$ is given by

$$\Gamma(\vec{x},t) = K[\gamma_{Na^+}\mathcal{C}_{Na^+}(\vec{x},t) + \gamma_{OH^-}\mathcal{C}_{OH^-}(\vec{x},t) + \gamma_{CH_3COO^-}\mathcal{C}_{CH_3COO^-}(\vec{x},t)]. \quad (7)$$

The charge conservation then gives

$$\mathcal{C}_{Na^+}(\vec{x},t) = \mathcal{C}_{OH^-}(\vec{x},t) + \mathcal{C}_{CH_3COO^-}(\vec{x},t), \quad (8)$$

so that if NaOH is denoted by $A$, $\Gamma$ is written

$$\Gamma(\vec{x},t) = K[(\gamma_{Na^+} + \gamma_{CH_3COO^-})\mathcal{C}_{Na^+}(\vec{x},t) + (\gamma_{OH^-} - \gamma_{CH_3COO^-})\mathcal{C}_A(\vec{x},t)], \quad (9)$$

and the fluctuations of $\mathcal{C}_A(\vec{x},t)$ are isolated by the probe only if the fluctuations of $\mathcal{C}_{Na^+}(\vec{x},t)$ can be neglected, which is sometimes possible, as will be seen in the later section on a moderate reaction.

The conductimeter used in the present experiment has been built in the L.S.G.C. of Nancy and extensively described by Grandjean et al. (1979). All the signals are sampled at a frequency of 3 kHz and stored on the disc of a Hewlett-Packard 1000 E series computer, therefore all statistical properties of the measured random field are numerically calculated.

## CHARACTERIZATION OF THE FLOW

### Grid Turbulence Without Injection

In this section, the essential properties of the fluctuating velocity field behind the grid are given. The mean velocity along the axis of the tunnel is 1.06 m $s^{-1}$, corresponding to a mesh Reynolds number (defined by $Re_M = \bar{U}_1 M/\nu$) of 35,000.

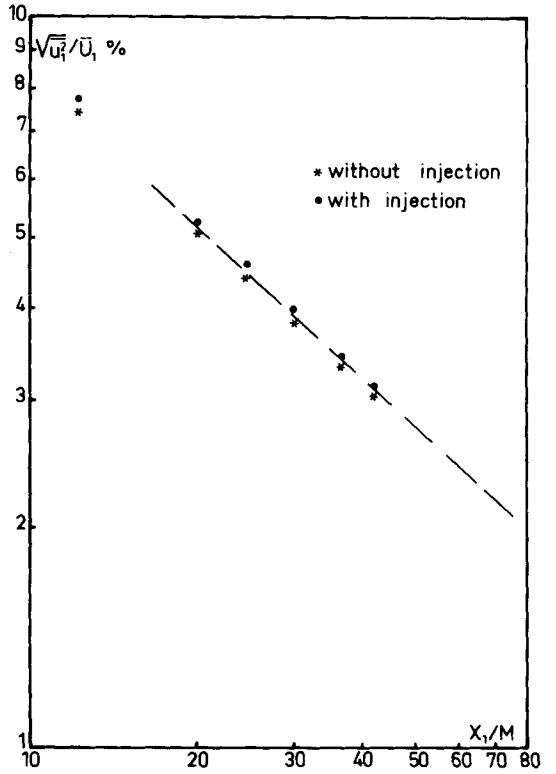


**Figure 3. Decay of $\sqrt{\overline{u_1^2}}/\bar{U}_1$ as a function of $X_1/M$ with and without injection.**

Without any injection through the grid, the variance $\overline{u_1^2}$ of the streamwise fluctuations is slightly greater than the variance of the transverse fluctuations (see Figure 2). This phenomenon is observed in all experiments concerning grid turbulence except for those of Comte-Bellot and Corrsin (1966), who placed a small contraction behind the grid in order to obtain better isotropy downstream. It can also be observed in Figure 2 that at a distance of 33 mesh lengths of downstream from the grid (that is, 33 $M$, where $M$ is the size of the grid mesh), the transverse variations of the principal Reynolds stress tensor components never exceed 10% inside a disk of radius 10 cm. The decay of the ratio $\overline{u_1^2}/\overline{U_1^2}$ vs. $X_1/M$ is given by the power law (Figure 3)

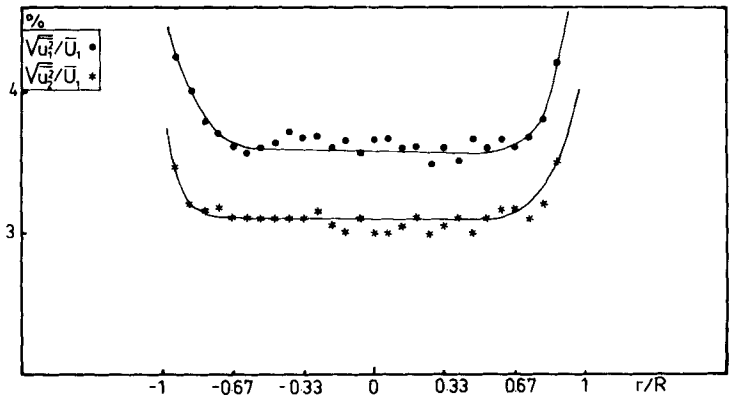


**Figure 2. Transverse variations of $\sqrt{\overline{u_1^2}}/\bar{U}_1$ and $\sqrt{\overline{u_2^2}}/\bar{U}_1$ (in the absence of injection) at a distance $X_1 = 33M$. ($R$ is the radius of the test section.)**

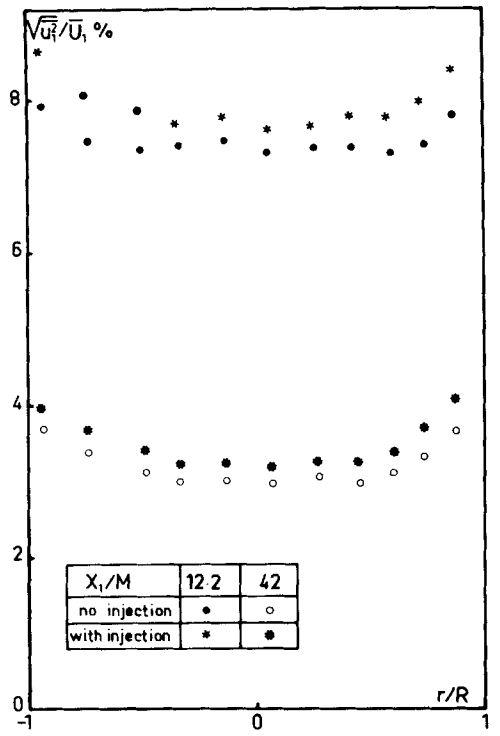


**Figure 4. Transverse variations of $\sqrt{\overline{u_1^2}}/\overline{U_1}$ with and without injection for $X_1/M$ = 12.2 and $X_1/M$ = 42. ($R$ is the radius of the test section.)**

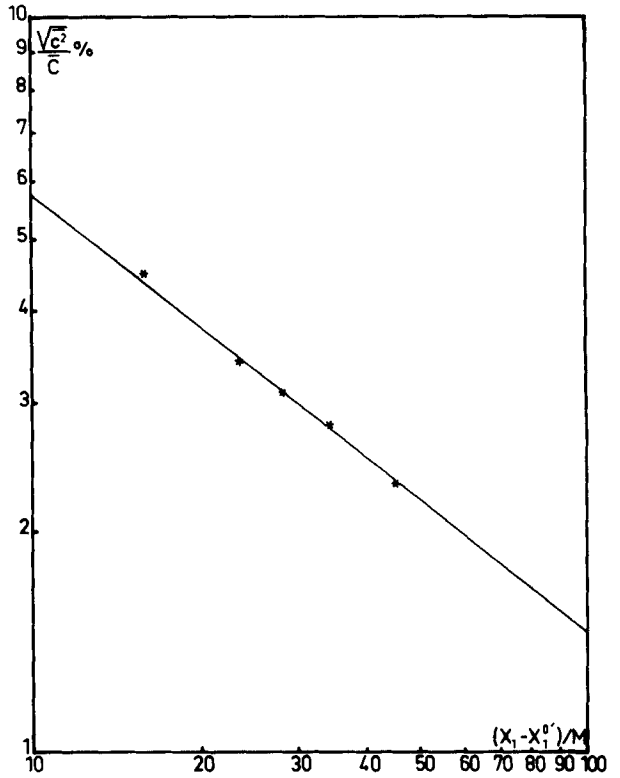


**Figure 5. Decay of $\sqrt{\overline{c^2}}/\overline{C}$ as a function of $X_1/M$ in the passive scalar case.**

$$\overline{u}_1^2/\overline{U}_1^2 = A' \left(\frac{X_1 - X_1^0}{M}\right)^{-n_u}, \qquad (10)$$

where $n_u$ has a value of 1.35, in agreement with Comte-Bellot and Corrsin's findings. The fictitious origin $X_1^0$ is to 3 $M$ and is selected to get an acceptable straight line through most of the data on logarithmic coordinates.

### Influence of Injection

The injection rate, defined as the ratio of the injected flow rate to that of the main flow, is chosen as 11%. In that case, the mean velocity downstream of the grid is equal to 0.7 m/s and the mesh Reynolds number to 24,500.

For a given value of $X_1/M$, it is observed that the turbulence level is greater than in the absence of injection (Figure 3). This phenomenon is probably linked to the energy production due to the shear introduced by the jets originating at the injectors, as noted by Gad El Hak and Corrsin (1974) in an analogous situation. It is, however, difficult to draw conclusions concerning the influence of the injection rate on the exponent $n_u$ of the power law of decay of $\overline{u}_1^2$ because the present experiment does not provide a large enough number of measurement points between 25 and 50 mesh lengths downsteam from the grid.

Finally, it is worthwhile to note that the homogeneity of the turbulence in planes parallel to the grid is not significantly affected by the injection, as observed in Figure 4.

## EVOLUTION OF A PASSIVE SCALAR

The passive scalar is a concentration field $\mathcal{C}$ of NaCl, as in the experiment of Gibson (1962). As indicated in Appendix 2, the injection setup is chosen so as to give the greatest possible value of the initial variance $\overline{c}^2$.

The mean concentration $\overline{C}$, which remains constant ($\overline{C}$ = 0,034 mol/L), is determined by a titration with a solution of silver nitrate.

The variance $\overline{c}^2$ of the concentration fluctuations proves to be a power law function of $X_1/M$ (Figure 5)

$$\frac{\overline{c}^2}{\overline{c}^2} = B' \left(\frac{X_1 - X_1^{0'}}{M}\right)^{-n_c}, \qquad (11)$$

where $n_c$ is equal to 1.3. The fictitious origin $X_1^{0'}$ is equal to $2M$ and therefore is different from $X_1^0$. Gibson also observed such a power law of decay but with $n_c$ equal to 1.5. Disregarding the fact that the number of measurement points is small in the present experiment and despite the large dispersion in the results of Gibson, the interpretation of such a discrepancy might be found in the work of Streenivasan et al. (1980). They have studied, in a grid turbulence, the evolution of a passive scalar represented by temperature fluctuations generated by the grid whose rods (or only part of them) are heated. When the distance $M_\theta$ between two heated rods is equal to $M$, it turns out that the mean value of $n_c$ is precisely 1.31. If, however, $M_\theta$ is equal to 2 $M$, $n_c$ proves to be equal to 1.55. The first situation corresponds approximately to the present experiment characterized by a large number of injectors distributed along the perimeter of each mesh, while the second is reminiscent of Gibson's injection setup, which is composed of just one injector per node.

From the decay laws, Eqs. 10 and 11, the Taylor scales $\lambda_g$ and $\lambda_c$ respectively associated with the velocity and concentration fluctuations are deduced according to the equations

$$\frac{d}{dt}\overline{u}_1^2 = -10\nu\overline{u}_1^2/\lambda_g^2 \qquad (12)$$

$$\frac{d}{dt}\overline{c}^2 = -12D\,\overline{c}^2/\lambda_c^2 \qquad (13)$$

(see, e.g, Sreenivasan et al., 1980), obtained in the theory of ho-

mogeneous and isotropic turbulence, where the one-point moments of the random quantities are time-dependent only. In the experiment, of course, all moments depend on $X_1$, and the intervals of the theory are linked to the space intervals by

$$\Delta t = \Delta X_1/\overline{U}_1 \tag{14}$$

in the part of the test section in which the turbulent field may be considered homogeneous, i.e., at a distance of about 30 mesh lengths downstream from the grid. This relation between time and space (Eq. 14), now classical for experimentalists working with homogeneous flows, will be used often in the present paper. Equations 10 to 13 give, then

$$\lambda_c^2 = \frac{12DM}{\overline{U}_1 n_c} \cdot \frac{X_1 - X_1^0}{M} \tag{15}$$

$$\lambda_g^2 = \frac{10\nu M}{\overline{U}_1 n_u} \cdot \frac{X_1 - X_1^0}{M}, \tag{16}$$

which implies

$$\lambda_c/\lambda_g = \frac{1}{\sqrt{Sc}}\sqrt{\frac{6}{5}\frac{n_u}{n_c}\frac{X_1 - X_1^0}{X_1 - X_1^0}}. \tag{17}$$

The observed values of $n_u$ and $n_c$ show that for sufficiently large $X_1$, this ratio is not very different from $(S_c)^{1/2}$, which confirms the comments made earlier concerning the evaluation of $\lambda_c$. As already noted, the conductimetric probe does not give a good measurement of the one-dimensional spectrum $G_c(K_1;X_1/M)$ associated with $\overline{c}^2$ for values of $K_1$ of the order of $\lambda_c^{-1}$. In particular, it has been verified that the Taylor scale obtained from the formula

$$\lambda_c(X_1/M) = \left\{\int_0^\infty K_1^2 \frac{G_C(K_1;X_1/M)}{\overline{c}^2(X_1/M)} dk_1\right\}^{-1/2} \tag{18}$$

is about eight times greater than the value deduced from Eq. 15.

## EVOLUTION OF A VERY SLOW ISOTHERMAL CHEMICAL REACTION

The reaction, which consists in the alkaline hydrolysis of ethyl acetate, is written

$$CH_3COOC_2H_5 + Na^+OH^- \rightarrow CH_3COO^-Na^+ + C_2H_5OH. \tag{19}$$

The kinetic constant is equal to 0.12 L/mol/s (Laidler, 1965).

Since a high level of concentrations fluctuations is required, the injected species has to be $Na^+OH^-$ denoted by $A$, the species $B$ being $CH_3COOC_2H_5$. As noted earlier, the conductivity of the fluid at point $\vec{x}$ and time $t$ is given by the relation

$$\Gamma(\vec{x},t) = K[(\gamma_{OH^-} - \gamma_{CH_3COO^-})\mathcal{C}_{OH^-}(\vec{x},t) + (\gamma_{Na^+} + \gamma_{CH_3COO^-})\mathcal{C}_{Na^+}(\vec{x},t)], \tag{20}$$

where the concentrations in $OH^-$ and $Na^+$ are different. The statistical average of the conductivity,

$$\overline{\Gamma}(x_1) = K[(\gamma_{OH^-} - \gamma_{CH_3COO^-})\overline{C}_{OH^-}(x_1) + (\gamma_{Na^+} + \gamma_{CH_3COO^-})\overline{C}_{Na^+}(x_1)], \tag{21}$$

is time-independent since the flow is statistically stationary. The concentration in $Na^+$ does not change under the influence of the reaction and therefore appears to be independent of $x_1$ at a distance of about 20 mesh lengths downsteam of the grid. Then the mean output voltage delivered by the conductimeter depends linearly on $\overline{C}_{OH^-}(x_1)$, which is equal to $\overline{C}_A(x_1)$.

The initial mean concentration $\overline{C}_A(o)$ is defined as the mean concentration that would exist in the test tunnel after a complete homogeneous dilution of species $A$ in the absence of any chemical reaction. If $C'_A$ denotes the concentration inside the tank containing $A$, and if $N$, $d$, and $S$ stand, respectively, for the number of injectors, their diameter, and the cross section of the tunnel it is clear that

$$\overline{U}_1 S\overline{C}_A(o) = U'_i \cdot N \cdot \pi \cdot \frac{d^2}{4} C'_A, \tag{22}$$

where $U'_i$ is the injection velocity. It implies

$$\overline{C}_A(o) = N \cdot \frac{\pi d^2}{4S}\frac{U'_i}{\overline{U}_1} C'_A. \tag{23}$$

The concentration $C'_A$ is obtained by acidimetry with a titrated solution 0.1 N of sulfuric acid.

The behavior of the ratio $\overline{C}_A/\overline{C}_A(0)$ as a function of $X_1/M$ (Figure 6) exhibits a slight decay, which is a mere consequence of the chemical reaction whose kinetic is governed in the mean by the following equation (the derivation is given in Appendix 1):

$$\frac{d}{dt}\overline{C}_A = \overline{U}_1\frac{d\overline{C}_A}{dX_1} = -K_r(\overline{C}_A \cdot \overline{C}_B + \overline{c_A c_B}) \tag{24}$$

A better understanding of the mechanisms involved requires the measurement of both $\overline{C}_B$ and $\overline{c_A c_B}$. This is, however, impossible at present. Instead, $\overline{C}_B$ was calculated from $\overline{C}_A$ using the fact that

$$\frac{d\overline{C}_A}{dt} = \frac{d\overline{C}_B}{dt}, \tag{25}$$

which implies

$$\overline{C}_B(t) = \overline{C}_A(t) + \overline{C}_B(o) - \overline{C}_A(o). \tag{26}$$

The definition of $\overline{C}_B(o)$ is identical to that of $\overline{C}_A(o)$ and its value is determined by back titration: An excess of sodium hydroxyde is added to a sample of ethyl acetate and the excess of hydroxyde is then titrated by acidimetry. (Here $\overline{C}_A(o)$ and $\overline{C}_B(o)$ are, respectively, equal to 0.09 and 0.06 mol/L.)

It is worthwhile comparing the evolution of $\overline{C}_A/\overline{C}_A(o)$ to the ideal behavior that would be obtained in a plug-flow reactor where the concentrations are uniform in each cross section. In that case the rate equations are

$$\frac{dC_A}{dt} = \frac{dC_B}{dt} = -K_r C_A C_B, \tag{27}$$

whose solution is

$$\frac{C_B(t)}{C_B(o)} = \frac{(1-\beta)\exp[-Kr(C_A(o) - C_B(o))t]}{1 - \beta\exp[-K_r(C_A(o) - C_B(o))t]}, \tag{28}$$

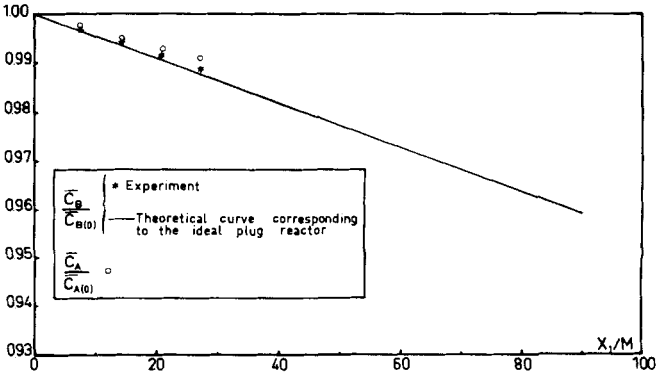


**Figure 6. Evoluton of the ratio $\overline{C}_B/\overline{C}_B(o)$ with $X_1/M$ and comparison with relation 28 in the case of a very slow reaction.**

where $\beta$ is defined by

$$\beta = C_B(o)/C_A(o). \tag{29}$$

The very small discrepancy appearing in Figure 6 between the above solution and the experimental points implies that

$$|\overline{c_A c_B}| \ll \overline{C}_A \cdot \overline{C}_B. \tag{30}$$

Consequently, in the case of a very slow reaction, the turbulent motion produces an ideal mixing and the situation is, in the mean, very similar to that observed in an ideal plug-flow reactor. Of course, such a conclusion does not hold close to the grid where the different species are still not mixed and where, as indicated in the Appendix 2, we have

$$\rho_{AB}(o) = -\frac{\overline{c_A c_B}(o)}{\overline{C}_A(o) \cdot \overline{C}_B(o)} = 1. \tag{31}$$

This ratio, introduced by Danckwerts (1952), gives a measure of the segregation level between the two species. At any point, the value of the above ratio is the result of two competitive mechanisms: a decrease of $\rho_{AB}$ due to turbulent mixing, which tends to bring both species into contact, and an increase of $\rho_{AB}$ associated with the chemical reaction, which enhances their segregation state. In the present experiment, the characteristic time associated with the chemical process can be evaluated as

$$\tau_R = \frac{1}{K_r \overline{C}_B(o)} \sim \frac{1}{K_r \overline{C}_A(o)} \sim 10^2 \text{s}. \tag{32}$$

On the other hand, the relaxation time $\tau_D$ associated with turbulent mixing in the vicinity of the grid is of the order of the time it takes the concentration of species $B$ to become uniform. Since the return toward uniformity is the consequence of turbulent diffusion of species $B$ in the jets, which is characterized by the following diffusion coefficient,

$$\nu_T = d\sqrt{\overline{q}^2}, \tag{33}$$

$\tau_D$ is given by

$$\tau_D \sim \frac{d^2}{\nu_T} \sim \frac{d}{\sqrt{\overline{q}^2}} \sim 4.10^{-2} \text{s}. \tag{34}$$

Here, $\overline{q}^2$ is evaluated at a distance of 10 meshes downstream the grid by extrapolating the curve in Figure 3. In view of the values of $\tau_R$ and $\tau_D$, it is obvious that the very fast turbulent mixing is the mechanism that explains the very small values of $|\overline{c_A c_B}|$ immediately behind the grid.

It is unfortunately impossible to obtain experimental data concerning the evolution of $\overline{c}_A^2$ since, as noted previously, the conductivity fluctuations result from a linear combination of concentration fluctuations associated with $\mathcal{C}_A$ and $\mathcal{C}_{Na^+}$ and no physical reasons permit the neglection of one of the two fluctuations. Moreover, as already noted, the frequency response of the conductimetric probe is not high enough to give information about the Taylor scale $\lambda_R$ associated with the $C_A$ fluctuations in the presence of the chemical reaction. Therefore it is impossible to deduce a precise value of the Damköhler number

$$Da_\lambda = \frac{K_r \overline{C}_B(o) \lambda_R^2}{D}. \tag{35}$$

Nevertheless, since the turbulence process is dominant in the present experiment, it is of course reasonable to admit that the order of magnitude of $\lambda_R$ is sensibly equal to $\lambda_c$ determined in the passive scalar case, so that $Da_\lambda$ is of the order of 0.1.

The injection configuration described in the following experiment makes it possible to neglect the concentration fluctuations of one of the species and therefore to use the conductimetric method in the measurement of the variance of the concentration fluctuations of the other one.

## EVOLUTION OF AN ISOTHERMAL MODERATE CHEMICAL REACTION

The reaction selected has consisted in the methylformate alkaline hydrolysis, which is written

$$HCOOCH_3 + Na^+OH^- \rightarrow HCOO^-Na^+ + CH_3OH, \tag{36}$$

and whose kinetic constant is equal to 47 L/mol/s (Brodkey, 1975).

In this new experiment, an aqueous solution of NaOH (species $A$) flows through the grid, while methylformate (species $B$) is injected. Such a choice, however unrealistic it might appear at first from previous remarks, is justified by the need to isolate the concentration fluctuations of species $A$. In addition, it turns out that this reaction produces fluctuations of $A$ that are high enough to insure reasonably good measurements. In the present case, the conductivity of the flow is given by

$$\Gamma(\vec{x}t) = K[(\gamma_{OH^-} - \gamma_{HCOO^-})\mathcal{C}_{OH^-(\vec{x},t)} + (\gamma_{Na^+} + \gamma_{HCOO^-})\mathcal{C}_{Na^+}(\vec{x},t)], \tag{37}$$

and according to the preceding section, the concentration in $Na^+$ is only very slightly affected by the grid and becomes uniform downstream after a time delay $\tau_D$ equal to 0.04 s, i.e., over a distance of about one mesh length. Then $Na^+$ concentration fluctuations are negligible in comparison with those of the other ions. Moreover, it can easily be checked using the conductimetric probe that there are no significant fluctuations of $\mathcal{C}_A$ in the absence of injection.

As in the foregoing section, the actual variation of the ratio $\overline{C}_A/\overline{C}_A(o)$ and of $\overline{C}_B/\overline{C}_B(o)$ with $X_1/M$ (Figure 7) is compared with its ideal plug flow behavior, which can be determined from Eq. 28. (As in the previous section, $\overline{C}_A(o) = 0.09$ mol/L and $\overline{C}_B(o) = 0.06$ mol/L.)

The discrepancy observed between the experiment and the relation in Eq. 28 shows that the correlation $\overline{c_A c_B}$ is significant. The evolution of the ratio $-\overline{c_A c_B}/\overline{C}_A\overline{C}_B$ deduced from Eq. 24 is given in Figure 8. This indicates that neither of the two competitive mechanisms (turbulent mixing and chemical reaction) described really dominates the other one. Their relative magnitude can be expressed in terms of a Damköhler number and evaluated from the following rate equation (see Appendix 1):

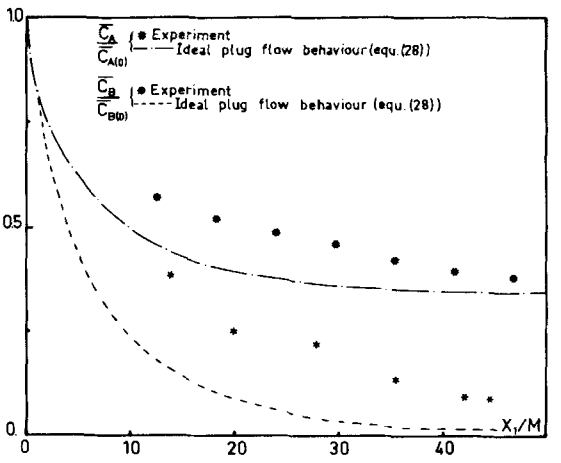


**Figure 7. Evolution of $\overline{C}_A/\overline{C}_A(o)$ and $\overline{C}_B/\overline{C}_B(o)$ with $X_1/M$ in the case of a moderate reaction. Comparison with the ideal plug flow behavior given by Eq. 28.**

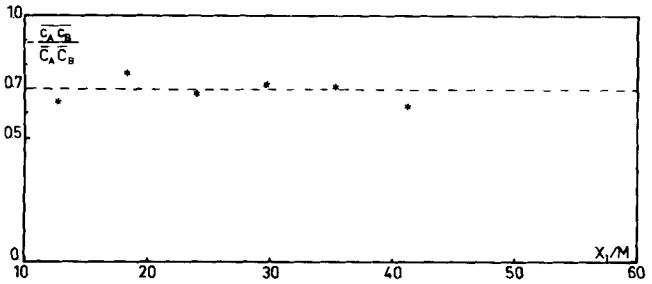


**Figure 8. The segregation coefficient $\rho_{AB}$ vs. $X_1/M$ in the moderate reaction case.**

$$\frac{d}{dt}\overline{c_A c_B} = -2D\frac{\partial c_A}{\partial X_K}\frac{\partial c_B}{\partial X_K} - K_r[(\overline{C}_A + \overline{C}_B)\overline{c_A c_B} + \overline{C}_A\overline{c}_B^2 + \overline{C}_B\overline{c}_A^2 + \overline{c_A^2 c_B} + \overline{c_B^2 c_A}]. \quad (38)$$

The variance destruction by molecular diffusion and the terms associated with the chemical reaction are, respectively, of the order of

$$D\overline{c_A c_B}/\lambda_R^2$$

and

$$-K_r(\overline{C}_A + \overline{C}_B)\overline{c_A c_B} \sim -Kr\overline{C}_A\overline{c_A c_B}, \quad (39)$$

since $\overline{C}_B$ is decaying to zero. Therefore, the Damköhler number

$$Da_\lambda = \frac{K_r\overline{C}_A(o)\lambda_R^2}{D} \quad (40)$$

is about 40 if it is assumed that $\lambda_R$ (which cannot be directly measured) is still equal to $\lambda_c$.

It is interesting to note at this point that the indirect evauation of $\overline{c_A c_B}$ reported here supports the view that Toor's model (1969) can be extrapolated to intermediate reaction rates, although it was originally designed for two extreme cases: very slow and very fast reactions. Indeed, Figure 9 shows that the decay of $|\overline{c_A c_B}|$ is similar to that of the variance of the passive scalar discussed earlier. The decay of $\overline{c}^2$, as that of $|\overline{c_A c_B}|$, is governed by diffusion, which probably explains the result.

The ratio $\overline{c}_A^2/\overline{C}_A^2(o)$, given in Figure 10 as a function of $X_1/M$, exhibits a maximum located at a distance of about 20 meshes

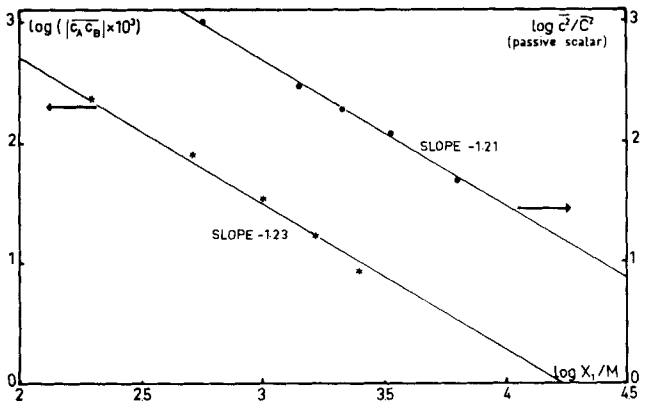


**Figure 9. Comparison of the decay of both the passive scalar variance and the correlation $|\overline{c_A c_B}|$.**

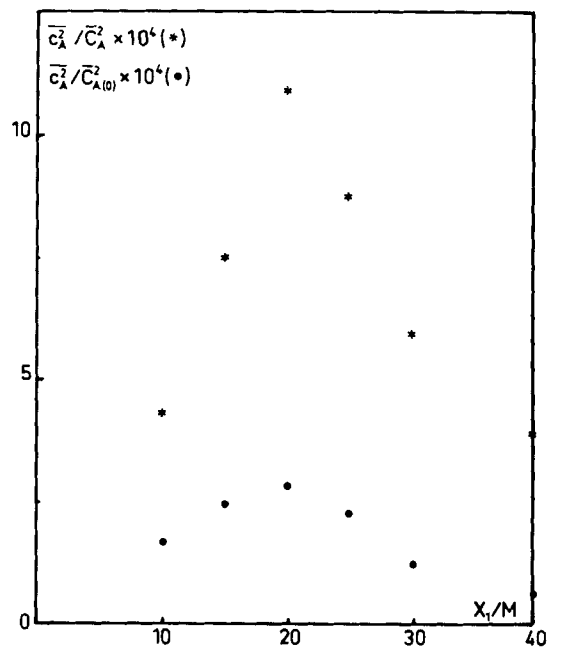


**Figure 10. Evolution of $\overline{c}_A^2/\overline{C}_A^2(o)$ and $\overline{c}_A^2/\overline{C}_A^2$ vs. $X_1/M$ in the moderate reaction case.**

downstream the grid. This evolution gives some information about the influence of the different terms in the righthand side of the rate equation for $\overline{c}_A^2$, which is written (Appendix 1)

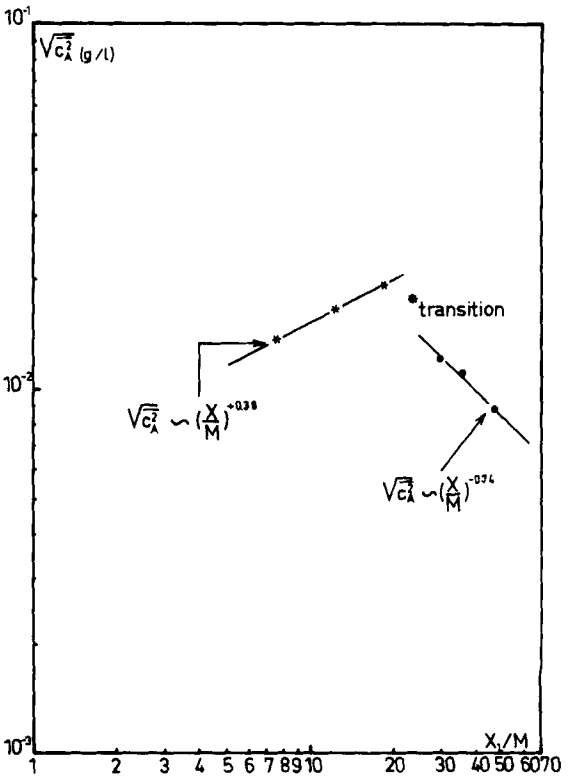


**Figure 11. Evolution of $\sqrt{\overline{c}_A^2}$ in a log-log plot. The second slope is not very different from that observed in Figure 5.**

$$\frac{d}{dt}\overline{c}_A^2 = -2D\,\overline{\frac{\partial c_A}{\partial X_K}\cdot\frac{\partial c_A}{\partial X_K}} - 2K_r[\overline{C}_A\overline{c_A c_B} + \overline{C}_B\overline{c}_A^2 + \overline{c_A^2 c_B}]. \tag{41}$$

If the triple correlation retains its sign, which is shown in Appendix 2, to be initially positive, the chemical term can be cut into

$$-2K_r\overline{C}_A\overline{c_A c_B} > o, \tag{42}$$

$$-2K_r(\overline{C}_B\overline{c}_A^2 + \overline{c_A^2 c_B}) < o. \tag{43}$$

In the first 20 mesh lengths downstream from the grid, expression 42 is dominant so that $\overline{c}_A^2$ is growing and reaches a maximum since $|\overline{c_A c_B}|$ is decaying. Expression 43 added to the term containing $D$ is then dominant and $\overline{c}_A^2$ exhibits a decay which, in the farthest sections of the duct, looks like that of a passive scalar (Figure 11).

## CONCLUSION

The main purpose of this work was to obtain experimental results concerning the evolution in the same field of quasiisotropic grid turbulence of both a passive concentration and an isothermal second-order reaction between two nonpremixed species $A$ and $B$. The behavior of the passive scalar field agrees well with that observed for temperature fluctuations in the same flow conditions, and these results complete those of Gibson obtained with a concentration field.

Two experiments in which a chemical reaction takes place have been carried out. The first one concerns a very slow reaction whose Damköhler number, $Da_\lambda$, is about 0.1. The main result is that the mean concentration field exhibits an ideal plug-flow reactor evolution so that the correlation $\overline{c_A c_B}$ is negligible against the product $\overline{C}_A\cdot\overline{C}_B$. In the second experiment, in which a faster reaction takes place, the ratio $-\overline{c_A c_B}/\overline{C}_A\overline{C}_B$ rapidly reaches a constant value of 0.7. This can be explained by an equilibrium between two competitive mechanisms: the turbulent destruction of $|\overline{c_A c_B}|$ by molecular diffusion and the chemical reaction that tends to remove the mixed species.

At this point, it is very important to note that the conductimetric method used here permits the measurement of the statistical properties of the concentration field of only one species. The properties of the other one have been indirectly deduced from the conservation equations. It is therefore crucial to develop new techniques that, at a given point of the flow, would provide simultaneous measurements of the fluctuations of the different concentration fields.


## ACKNOWLEDGMENT

The authors wish to express their deep appreciation to J. Villermaux (L.S.G.C. of Nancy) for his interest in the work and for suggesting the particular chemical reactions that were chosen. Also fruitful discussion with J. Bataille are gratefully acknowledged, and J. Tichy assisted in polishing the English. This work was supported by the Centre National de la Recherche Scientifique.


## NOTATION

$A,B$ = different reacting species
$A',B'$ = constants
$\mathcal{C}$ = instantaneous passive scalar concentration at point $\vec{x}$
$\overline{C}$ = mean concentration of a passive scalar at point $\vec{x}$
$c$ = instantaneous passive scalar concentration fluctuation at point $\vec{x}$
$\mathcal{C}_\alpha$ = instantaneous concentration of species $\alpha$ at point $\vec{x}$
$\overline{C}_\alpha$ = mean concentration of species $\alpha$ at point $\vec{x}$
$c_\alpha$ = instantaneous concentration fluctuation of species $\alpha$ at point $\vec{x}$
$C$ = characteristic concentration
$\overline{c_A c_B}$ = one-point double correlation between concentration fluctuations of species $A$ and $B$
$\overline{c}_A^2$ = variance of concentration fluctuations of species $A$
$\overline{c_A^2 c_B}$ = one-point triple correlation between concentration fluctuations of species $A$ and $B$
$C'_A$ = uniform concentration of species $A$ in the tank upstream of the injectors
$d$ = injector diameter
$\mathcal{D}$ = characteristic radius of the conductimetric probe
$D$ = molecular diffusivity
$Da_\lambda$ = Damköhler number based on Taylor's length scale
$G_c$ = one-dimensional energy spectrum of the passive scalar concentration fluctuations
$K_1$ = component of the wave vector in the $X_1$ direction
$K_r$ = chemical reaction kinetic constant
$L$ = length scale of the energy-containing eddies
$M$ = mesh length of the grid
$M_\theta$ = distance between two heated rods in the experiment of Streenivasan et al. (1980)
$N$ = number of injectors
$n_u$ = exponent of the power law of decay of the variance associated with the velocity fluctuations in the $X_1$ direction
$n_c$ = exponent of the power law of decay of the variance associated with the passive scalar concentration fluctuations
$\overline{q}^2$ = fluctuating motion kinetic energy
$Re_L$ = Reynolds number based on the length scale of the energy containing eddies and on the fluctuating motion kinetic energy
$Re_M$ = Reynolds number based on the mesh length and on the streamwise mean velocity
$Sc$ = Schmidt number
$S$ = area of the water tunnel cross section
$t$ = time
$\overline{U}_1$ = streamwise mean velocity
$U'_i$ = injection velocity
$\overline{u_i^2}$ = variance of the velocity fluctuations in the $X_i$ direction
$X_1$ = streamwise coordinate
$X_2$ = vertical coordinate
$X_1^0$ = fictitious origin used in the decay law for the variance of the velocity fluctuations
$X_1^{0'}$ = fictitious origin used in the decay law for the variance of the passive scalar concentration fluctuations
$Z_\alpha$ = charge of species $\alpha$

### Greek Letters

$\alpha'$ = constant
$\beta$ = Stoichiometric ratio
$\gamma_\alpha$ = mobility of species $\alpha$
$\Gamma$ = instantaneous conductivity of the fluid mixture at point $\vec{x}$
$\Delta$ = difference
$\lambda_c$ = passive scalar Taylor's length scale
$\lambda_g$ = velocity field Taylor's length scale
$\lambda_R$ = reacting species Taylor's length scale
$\nu$ = kinematic viscosity
$\nu_T$ = turbulent diffusion coefficient
$\tau$ = characteristic time scale

## APPENDIX 1

In what follows, we consider an incompressible fluid mixture containing two reacting species A and B having the same constant molecular diffusivity $D$. The chemical reaction is of the second order and is assumed to be isothermal. The kinetic constant is denoted by $K_r$.

The conservation equations governing the evolution of the velocity and concentration fields are written

$$\frac{\partial U_i}{\partial t} + U_j \frac{\partial U_i}{\partial X_j} = -\frac{1}{\rho}\frac{\partial P}{\partial X_i} + \nu \frac{\partial^2 U_i}{\partial X_K^2}, \tag{44a}$$

$$\partial U_i / \partial X_i = 0; \tag{44b}$$

$$\frac{\partial \mathcal{C}_A}{\partial t} + U_j \frac{\partial \mathcal{C}_A}{\partial X_j} = D \frac{\partial^2 \mathcal{C}_A}{\partial X_K^2} - K_r \mathcal{C}_A \mathcal{C}_B, \tag{44c}$$

$$\frac{\partial \mathcal{C}_B}{\partial t} + U_j \frac{\partial \mathcal{C}_B}{\partial X_j} = D \frac{\partial^2 \mathcal{C}_B}{\partial X_K^2} - K_r \mathcal{C}_A \mathcal{C}_B. \tag{44d}$$

If the flow is turbulent, these fields are random and, as usual, are split into an averaged and a fluctuating part, so that

$$U_i = \overline{U}_i + u_i, \tag{45a}$$

$$\mathcal{C}_\alpha = \overline{C}_\alpha + c_\alpha. \tag{45b}$$

If the case of a general inhomogeneous turbulent flow, Patterson (1981) deduced the following equations for $\overline{C}_A$, $\overline{c_A^2}$, $\overline{c_A c_B}$:

$$\frac{\partial \overline{C}_A}{\partial t} + \overline{U}_j \frac{\partial \overline{C}_A}{\partial X_j} + \frac{\partial}{\partial X_j}\overline{(u_j c_A)} = D \frac{\partial^2 \overline{C}_A}{\partial X_K^2} - K_r(\overline{C}_A \overline{C}_B + \overline{c_A c_B}), \tag{46a}$$

$$\frac{\partial}{\partial L}\overline{c_A^2} + \overline{U}_j \frac{\partial \overline{c_A^2}}{\partial X_j} + \frac{\partial}{\partial X_j}\overline{(u_j c_A^2)} + 2\overline{u_j c_A}\frac{\partial}{\partial X_j}\overline{C}_A = -2D\overline{\frac{\partial c_A}{\partial X_K}\frac{\partial c_A}{\partial X_K}} + 2D \cdot \frac{\partial^2 \overline{c_A^2}}{\partial X_K^2} - 2K_r(\overline{C}_A \overline{c_A c_B} + \overline{C}_B \overline{c_A^2} + \overline{c_A^2 c_B}), \tag{46b}$$

$$\frac{\partial}{\partial t}\overline{c_A c_B} + \overline{U}_j \frac{\partial}{\partial X_j}\overline{c_A c_B} + \frac{\partial}{\partial X_j}\overline{(u_j c_A c_B)} + \overline{u_j c_B} \cdot \frac{\partial \overline{C}_A}{\partial X_j} + \overline{u_j c_A} \cdot \frac{\partial \overline{C}_B}{\partial X_j} = D\overline{\frac{\partial^2 c_A c_B}{X_K^2}} - 2D\overline{\frac{\partial c_A}{\partial X_K}\frac{\partial c_B}{\partial X_K}} - K_r[(\overline{C}_A + \overline{C}_B)\overline{c_A c_B} + \overline{C}_A \overline{c_B^2} + \overline{C}_B \overline{c_A^2} + \overline{c_A^2 c_B} + \overline{c_B^2 c_A}]. \tag{46c}$$

Analogous equations are obtained for $\overline{C}_B$ and $\overline{c_B^2}$ by permutations of $A$ and $B$ in Eqs. 46a and 46b.

In the particular case of our experiment, the turbulent flow is isotropic, which implies

$$\overline{u_j c_A} = \overline{u_j c_A^2} = \overline{u_j c_A c_B} = o. \tag{47}$$

Moreover, the flow is steady and homogeneous in the planes paralle to the grid so that all moments of the concentration fields depend on $X_1$ only. The preceding equations reduce to

$$\overline{U}_1 \frac{\partial \overline{C}_A}{\partial X_1} = D \frac{\partial^2 \overline{C}_A}{\partial X_1^2} - K_r(\overline{C}_A \overline{C}_B + \overline{c_A c_B}), \tag{48a}$$

$$\overline{U}_1 \frac{\partial \overline{c_A^2}}{\partial X_1} = 2D \frac{\partial^2 \overline{c_A^2}}{\partial X_1^2} - 2D\overline{\frac{\partial c_A}{\partial X_K}\frac{\partial c_A}{\partial X_K}} - 2K_r(\overline{C}_A \overline{c_A c_B} + \overline{C}_B \overline{c_A^2} + \overline{c_A^2 c_B}), \tag{48b}$$

$$\overline{U}_1 \frac{\partial}{\partial X_1}\overline{c_A c_B} = D \frac{\partial^2}{\partial X_1^2}\overline{(c_A c_B)} - 2D\overline{\frac{\partial c_A}{\partial X_K}\frac{\partial c_B}{\partial X_K}} - K_r[(\overline{C}_A + \overline{C}_B)\overline{c_A c_B} + \overline{C}_A \overline{c_B^2} + \overline{C}_B \overline{c_A^2} + \overline{c_A^2 c_B} + \overline{c_B^2 c_A}]. \tag{48c}$$

As the Reynolds number and the Schmidt number are much greater than 1, the diffusion effects along $X_1$ are negligible in the equations for $\overline{C}_A$ and $\overline{c_A^2}$, which become

$$\overline{U}_1 \frac{\partial \overline{C}_A}{\partial X_1} = -K_r(\overline{C}_A \overline{C}_B + \overline{c_A c_B}), \tag{49a}$$

$$\overline{U}_1 \frac{\partial \overline{c_A^2}}{\partial X_1} = -2D\overline{\frac{\partial c_A}{\partial X_K}\frac{\partial c_A}{\partial X_K}} - 2K_r(\overline{C}_A \overline{c_A c_B} + \overline{C}_B \overline{c_A^2} + \overline{c_A^2 c_B}). \tag{49b}$$

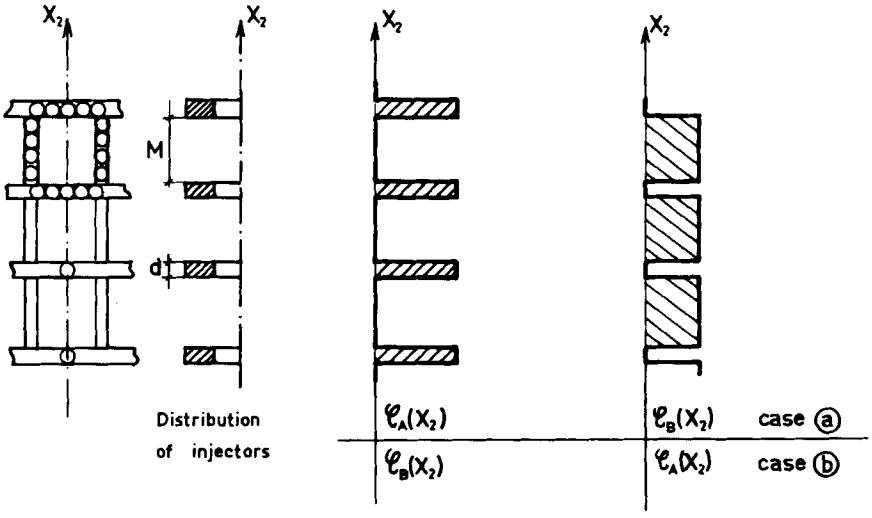


**Figure 12. The ideal distribution of the fields $\mathcal{C}_A(X_2)$ and $\mathcal{C}_B(X_2)$ along $X_2$.**

Finally, if the Taylor scale $\lambda_R$ associated with the fluctuating concentration field $c_A$ is introduced, it may be written, as indicated by Tennekes and Lumley (1972),

$$-2D\overline{\frac{\partial c_A}{\partial X_K}\cdot\frac{c_A}{\partial X_K}} = -12D\frac{\bar{c}_A^2}{\lambda_R^2} \tag{50}$$

so that we also have

$$\overline{U}_1\frac{\partial \bar{c}_A^2}{\overline{X}_1} = -12D\frac{\bar{c}_A^2}{\lambda_R^2} - 2K_r(\overline{C}_A\overline{c_Ac_B} + \overline{C}_B\bar{c}_A^2 + \overline{c_A^2c_B}). \tag{51}$$

## APPENDIX 2

In order to discuss the influence of the injected species on some statistical properties of the different concentration fields, an elementary one-dimensional model is considered to describe the concentration fields along the $X_2$ axis indicated in Figure 12 in the plane containing the outlet sections of the injectors. The latter, having a diameter equal to $d$, are regularly distributed along the $X_2$ axis from $-\infty$ to $+\infty$. The distance between two successive injectors is equal to $M$, which corresponds to the grid mesh as indicated in Figure 12.

If $\mathcal{C}_\alpha(X_2)$ is the concentration field of species $\alpha$, its spatial average $\overline{C}_\alpha$ along $X_2$ is defined as

$$\overline{C}_\alpha = \lim_{\mathcal{L}\to\infty}\frac{1}{\mathcal{L}}\int_{-\mathcal{L}}^{+\mathcal{L}}\mathcal{C}_\alpha(X_2)dX_2. \tag{52}$$

If we consider two species $A$ and $B$, and if $A$ is injected, $B$ being diluted in the main flow (case $a$ in Figure 12), the field $\mathcal{C}_A(X_2)$ is equal to

$$\overline{C}_A\left(\frac{M}{d}+1\right)$$

in the outlet cross section of the injectors.

On the contrary, $\mathcal{C}_B(X_2)$ is equal to zero in this latter region and equal to

$$\overline{C}_B\left(\frac{d}{M}+1\right)$$

between two successive injectors.

As the two fields are not mixed, it is clear, in particular, that

$$\overline{\mathcal{C}_A(X_2)\mathcal{C}_B}(X_2) = o, \tag{53}$$

$$\overline{\mathcal{C}_A^2(X_2)\mathcal{C}_B}(X_2) = o. \tag{54}$$

Splitting $\mathcal{C}_\alpha(X_2)$ ($\alpha = A$ or $B$) into a mean and a fluctuating part as

$$\mathcal{C}_\alpha(X_2) = \overline{C}_\alpha + c_\alpha(x_2), \tag{55}$$

Eq. 53 implies

$$\overline{c_Ac_B} = -\overline{C}_A\cdot\overline{C}_B, \tag{56}$$

which gives

$$\rho_{AB} = \frac{-\overline{c_Ac_B}}{\overline{C}_A\cdot\overline{C}_B} \tag{57}$$

Moreover, by use of Eq. 56, Eq. 54 gives

$$\overline{c_A^2c_B} = \overline{C}_B\overline{C}_A^2(1-\bar{c}_A^2/\overline{C}_A^2). \tag{58}$$

It is obvious that when $A$ is injected case $a$ in Figure 12), we have

$$\frac{\bar{c}_A^2}{\overline{C}_A^2} = \frac{M}{d} > 1, \tag{59}$$

which implies according to Eq. 58

$$\overline{c_A^2c_B} < o. \tag{60}$$

On the contrary, when $A$ is diluted in the main flow (case $b$ in Figure 12), it may be written

$$\frac{\bar{c}_A^2}{\overline{C}_A^2} = \frac{d}{M} < 1, \tag{61}$$

implying

$$c_A^2c_B > o. \tag{62}$$

Of course, all these conclusions are true when the concentration fields are averaged along $X_2$. However, it may be assumed that under the influence of the turnover effect of the turbulence, such a similar statistical state will be observed along the $X_1$ axis in the grid vicinity.

## LITERATURE CITED


Alcaraz, E., and J. Mathieu, "Réalisation d'une soufflerie à haut niveau de turbulence," *C.R.A.S. Paris*, **261**, 2,435 (1965).

Bennani A., E. Alcaraz, and J. Mathieu, "An Experimental Setup for Interaction Turbulence Chemical Reaction Research," *Int. J. Heat Mass Transfer*, **24**, 1549 (1981).

Brodkey, R. S., *Turbulence in Mixing Operations Theory and Application to Mixing and Reaction*, Academic Press, New York (1975).

Comte-Bellot, G., and S. Corrsin, "The Use of a Contraction to Improve the Isotropy of Grid Generated Turbulence," *J. Fluid Mech.*, **48**, 657 (1966).

Corrsin, S., "Turbulent Flow, Experimental Methods," *Handbuch der Physik*, S. Flugge and C. Truedell, Eds., Springer, **8**, Pt. 2, 524 (1963).

Danckwerts, P. V., "The Definition and Measurement of Some Characteristics of Mixtures," *Appl. Sci. Res.*, **A3**, 279 (1952).

Gad El Hak, M., and S. Corrsin, "Measurements of Nearly Isotropic Turbulence Behind a Uniform Jet Grid," *J. Fluid Mech.*, **62**, 115 (1974).

Gibson, C. H., "Scalar Mixing in Turbulent Flow," Ph.D. Thesis, Stanford Univ. (1962).

Gibson, C. H., and W. H. Schwartz, "Detection of Conductivity Fluctuation in a Turbulent Flow Field," *J. Fluid Mech.*, **16**, 365 (1963).

Grandjean, C., et al., *J. Electrochim.*, Strasbourg (June, 1979).

Hill, J. C. "Homogeneous Turbulent Mixing with Chemical Reaction," *Ann. Rev. Fluid Mech.* (1976).

Laidler, *Chemical Kinetics*, 2nd ed., McGraw-Hill, New York (1965).

Patterson, G. K. "Application of Turbulence Fundamentals to Reactor Modeling and Scaleup," *Chem. Eng. Commun.*, **8**, 25 (1981).

Sreenivasan, K. R., et al., "Temperature Fluctuation and Scale in Grid-Generated Turbulence," *J. Fluid Mech.*, **100**, 597 (1980).

Tennekes, H., and J. L. Lumley, *A First Course in Turbulence*, MIT Press, Cambridge, MA (1972).

Toor, H. L., "Turbulent Mixing of Two Species With and Without Chemical Reaction," *Ind. Eng. Chem. Fund.*, **8**, (4) 655 (1969).

Villermaux, J., "Mixing in Chemical Reactors," *I.S.C.R.E.*, Boston, no. 7 (Oct., 1982).



*Manuscript received Jan. 3, 1984; revision received July 31, 1984, and accepted Aug. 17.*